International Journal of Modern Physics C
Vol. 17, No. 3 (2006) 419–434

THE ROLE OF PANIC IN THE ROOM EVACUATION PROCESS

DANIEL R. PARISI* and CLAUDIO O. DORSO†

Departamento de Física-Facultad de Ciencias Exactas y Naturales
Universidad de Buenos Aires, Pabellón 1 Ciudad Universitaria
1428 Buenos Aires, Argentina
* *dparisi@df.uba.ar*
† *codorso@df.uba.ar*

In the present work we studied the room evacuation problem using the social force model introduced by Helbing and coworkers. The "faster is slower" effect induced by panic was analyzed. It could be explained in terms of increasing mean clogging delays which shows a strong correlation with certain structures that we call "blocking clusters". Also a steady state version of the problem was implemented. It shows that, from a macroscopic point of view, the optimal evacuation efficiency correspond to the state at which the difference between the system desire force minus the system granular force is maximum.

Keywords: Panic evacuation; social force model; discrete pedestrian simulation.

PACS Nos.: 45.70Vn, 34.10.+x, 89.65.Lm.

1. Introduction

The problem of evacuation of pedestrians from a room under panic conditions is of obvious importance in common life. In past years, several computer models that simulate pedestrian dynamics were developed.[1] These codes do not take into account the effect of panic on the pedestrian behavior.

Pedestrian flow through a bottleneck[2] and clogging in a T-shape channel[3] have been studied previously using the lattice-gas model of biased random walkers. More general self driven particle systems with simple interactions were studied by Vicsek,[4] Albano[5] and Czirók.[6] Phase transitions were found for these systems.

The evacuation through a narrow door during an emergency is a complex problem not well-understood yet, that can cause very dramatic blocking effects.

A model that takes into account panic is the so-called "Social Force Model" proposed by Helbing and Molnar.[7] This model considers the discrete nature of the "pedestrian fluid", allowing us to fix the physical parameters of each individual (mass, shoulder width, desired velocity, target, etc.). Real scale interaction forces can be calculated, in particular, the contact forces which may cause high pressures capable of pushing down a wall of bricks or to asphyxiate people in the crowd. The above characteristics cannot be properly taken into account with cellular automata approaches or traditional models using continuous fluid approximations.

The understanding of the evacuation dynamics will allow the design of more comfortable and safe pedestrian facilities.

Also, special devices that speed up the evacuation processes could be investigated. A simple example is to place a column near the exit as proposed by Helbing *et al.*[8] More sophisticated devices could be developed based on a validated dynamical under panic model.

The aim of the present paper is to investigate the microscopic mechanisms involved in the room evacuation process. First we analyze the behavior of a crowd composed of a fixed initial number of pedestrians until complete evacuation is attained. This process is nonstationary. The number of pedestrians inside the room is a function of time as well as pressure and other dynamical properties of the system. We then focus on a stationary problem. In this case the state of maximum jamming is maintained along the time by reinserting outgoing particles into the room. This stationary situation allows us to study some features that cannot be revealed in the nonstationary case.

This work is organized as follows. In Sec. 2, we present the "Social Force Model" proposed by Helbing *et al.*[8] In Sec. 3, we describe the simulations made. In Sec. 4, we introduce some definitions that allow the proper characterization of relevant observables. In Sec. 5, we summarize the results for the nonstationary problem. In Sec. 6, the results of the stationary case are presented. Finally in Sec. 7, we present our conclusions.

2. The Model

In this work we use the "Social Force Model" proposed by Helbing and coworkers.[8] In this model the dynamics of each particle (p_i) is driven by three forces with different properties. They are: "Desire Force" ($\mathbf{F}_{Di}$), "Social Force" ($\mathbf{F}_{Si}$) and "Granular Force" ($\mathbf{F}_{Gi}$). The corresponding expressions are:

$$\mathbf{F}_{Di} = m_i \frac{(v_{di}\mathbf{e}_i - \mathbf{v}_i)}{\tau} \, . \tag{1}$$

In this equation, m_i is the particle mass, v_i and v_{di} are the actual and desired velocities respectively, $\mathbf{e}_i$ is the versor pointing to the desired target (particles inside the room have their targets located at a random position in the exit door), and τ is a constant related with the relaxation time of the particle to achieve v_d.

$$\mathbf{F}_{Si} = \sum_{j=1, j\neq i}^{N_p} A \exp\left(\frac{-\epsilon_{ij}}{B}\right) \mathbf{e}^n_{ij} \, . \tag{2}$$

N_p is the total number of pedestrians in the system, A and B are constants that determine the strength and range of the social interaction, and $\mathbf{e}^n_{ij}$ is the versor pointing from particle p_j to p_i. This direction is the "normal" direction between two particles.

$$\mathbf{F}_{Gi} = \sum_{j=1, j\neq i}^{N_p} [(-\epsilon_{ij} k_n - \gamma \mathbf{v}_{ij}^n)\mathbf{e}_{ij}^n + (\mathbf{v}_{ij}^t \epsilon_{ij} k_t)\mathbf{e}_{ij}^t] g(\epsilon_{ij}) , \quad (3)$$

with

$$\epsilon_{ij} = r_{ij} - (R_i + R_j) . \quad (4)$$

Here the tangential versor ($\mathbf{e}_{ij}^t$) indicates the corresponding perpendicular direction, r_{ij} is the distance between the centers of p_i and p_j, R is the particle radius, k_n and k_t are the normal and tangential elastic restorative constants, γ is the damping constant (the Helbing original model did not consider the nonconservative term associated with this constant), v_{ij}^n is the normal projection of the relative velocity seen from p_j ($\mathbf{v}_{ij} = \mathbf{v}_i - \mathbf{v}_j$), v_{ij}^t is the tangential projection of the relative velocity, and the function $g(\epsilon_{ij})$ is $g = 1$ if $\epsilon_{ij} < 0$ or $g = 0$ otherwise. Particle positions were initially uniformly distributed inside the room in such a way that $\epsilon_{ij} > 0$ for all pairs ij. Also initial velocities were randomly generated inside the range 1.0 ± 0.005 m/s.

The interaction of particles with walls and vertex through social and granular forces are computed in an analogous way.

3. Numerical Simulations

In order to explore the room evacuation dynamics with the model described above, we have performed a series of numerical simulations varying v_d.

Following Helbing, the model parameters used were $\tau = 0.5$ s, $A = 2000$ N, $B = 0.08$ m, $k_n = 1.2\ 10^5$ N/m, $k_t = 2.4\ 10^5$ kg/m/s, $m = 80 \pm 10$ kg and $\gamma = 100$ kg/s.

The geometry of the room was a 20 m by 20 m square with an exit door of width $L = 1.2$ m. Pedestrians shoulder widths were uniformly distributed between (0.5 m, 0.58 m). In all the simulations we have fixed the size of the crowd to be 200 individuals.

3.1. *Nonstationary simulations*

As stated above, the problem of room evacuation is a nonstationary process. As time goes by and pedestrians leave the room, the conditions of density and pressure inside the room change. In this calculation we investigated the whole process of evacuation (i.e., until all individuals have left the room), performing a series of runs for each of the following values of v_d: 0.8, 1.0, 1.5, 1.75, 2.0, 2.25, 2.5, 3.0, 3.5, 4.0, 5.0, 6.0 and 8.0 m/s. In each case the desired velocities for the 200 particles were uniformly distributed inside a range of $v_d \pm 0.05$ m/s.

The complete results for this nonstationary case were published in a previous work.[9] Here the main results will be revisited.

3.2. *Stationary simulations*

It is quite intuitive that the rate at which the room is evacuated is somehow related to the pedestrian jamming in the inner neighborhood of the exit door. This effect, which we fully describe below, is difficult to study in the nonstationary case because it lasts for a short time. In view of this difficulty we have implemented a stationary case in which the jamming effects remain constant in time. This has been accomplished by reinserting particles that have left the room, back inside of it. Outgoing pedestrians that have reached 3 m away from the door are instantaneously placed inside the room at a random position not closer than 1.5 m from any other pedestrian.

Steady state simulations were performed for the following values of v_d: 0.8, 1.0, 1.125, 1.25, 1.375, 1.5, 1.75, 2.0, 2.25, 2.5, 3.0, 4.0, 6.0 and 8.0 m/s. The simulation time, in all cases, was 1000 seconds.

4. Some Definitions

In this section we introduce the definitions of those magnitudes which we have found useful in order to properly explore the systems' properties.

4.1. *Clogging delay*

Pedestrians trying to leave a room can generate high pressures and densities in the neighborhood of the exit door. In such a case, it might happen that a group of pedestrian gets interlocked, for a more or less short period of time, at the exit door, thus becoming obstacles to other pedestrians. This effect is known as clogging and we name "clogging delay" (*cd*) as the period of time between two individuals that leave the room consecutively. In the discharge curve (the number of individuals that have left the room as a function of time) clogging delays show up as horizontal segments of the curve (see Fig. 2). Depending on the value of v_d, only social forces (low v_d) or social plus granular forces (high v_d) will be the dominating interactions. Hence, there are two kinds of clogging delays that we call social delay and granular delay, depending on the strength of the granular interaction between particles.

4.2. *Granular cluster*

We define a "granular cluster" (C_g) in the following way. Given a particle p_i of radius R_i and a cluster C_g,

$$p_i \epsilon C_g \Leftrightarrow \exists\ p_j \epsilon C_g / r_{ij} < (R_i + R_j)\,, \tag{5}$$

where (p_j) indicates the jth particle (or person) and R_j is his radius. This means that, C_g is a set of particles that interact not only with social and desire forces, but also with granular forces.

4.3. *Blocking cluster*

Just before the exit, the contact forces are able to produce arch-like blocking clusters (see Fig. 4).

A "blocking cluster" (C_{bc}) is defined as the subset of clusterized particles closest to the door whose first and last component particles are in contact with the walls at both sides of the door.

These blocking clusters can be more or less stable and can last up to six seconds in our simulations and they can be composed of three to more than ten particles.

5. The Evacuation Process (Nonstationary Case)

In this section the evacuation of 200 pedestrian from a room is investigated. This process is clearly nonstationary since, as a function of time, the number of particles inside the room is reduced and as a consequence, the number of particles pushing each other near the exit door diminishes. This means that the state of the system is changing with time, which makes it difficult to properly characterize it. One variable that characterizes the evolution of the system is the evacuation time for all the considered pedestrians.

5.1. *Evacuation time versus desired velocity*

Helbing and coworkers have analyzed different properties of the model described in Sec. 2. In what is relevant to this work they have shown that, in the room evacuation problem, the total evacuation time curve has a typical functional behavior, displaying a minimum at moderate values of v_d. We will denote this minimum as the desired velocity threshold v_{dt}. For velocities above and below, the evacuation time increases, which means that a very interesting phenomenon takes place. Above the threshold, the larger the value of v_d, the longer it takes for the individuals to evacuate a room.

The importance of such a behavior is clear if one thinks about situations in which the crowd is in a state of panic. A state of panic is associated with high values of v_d i.e., individuals try to move faster and faster towards the exit door. When we analyze the evacuation time in our simulations the behavior described by Helbing is recovered. In Fig. 1 we show such a curve.

5.2. *Discharge curve*

Further information can be gained if we look at the discharge curve, i.e., the number of particles that have left the room as a function of time. In this curve, horizontal lines denote the time difference between two successive particles which leave the room. These time differences will be referred to as "delays" (as stated above and see next section). In Fig. 2, we show this curve for a single realization at three different values of v_d, namely 0.8, 2.0 and 6.0 m/s.

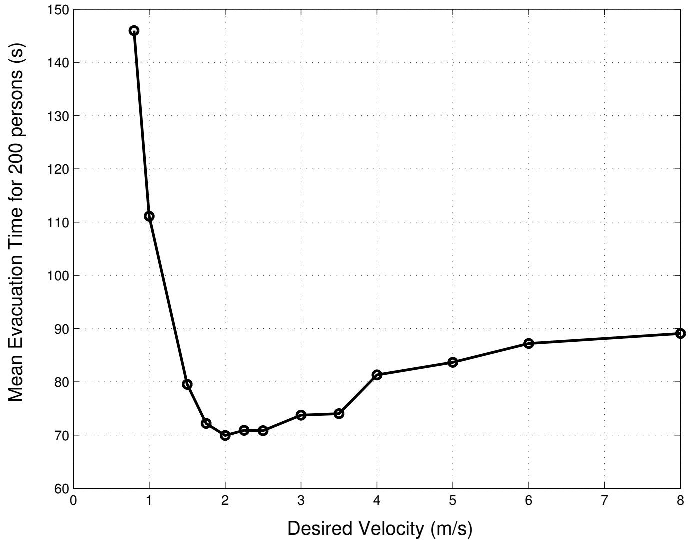

Fig. 1. Mean evacuation time as a function of the v_d for all the 200 persons.

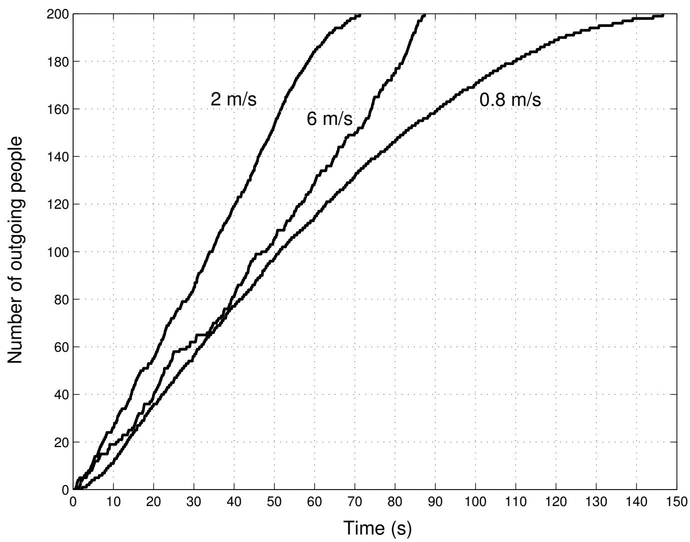

Fig. 2. This figure shows the so-called discharge curve i.e., the time at which each particle leaves the room. This curves are calculated from a single simulation for three different values of v_d, namely 0.8, 2.0 and 6.0 m/s. Note that the curve corresponding to the highest v_d has a less smooth shape. This is related to the presence of large clogging delays (see text).

It can be easily recognized that at larger values of v_d, the occurrence of abnormally large delays becomes more probable, particularly in the intermediate stages of the evolution of the system (there is a rather large fraction of the total number of particles inside the room).

The flow rate is the derivative of the discharge curve. It is easy to realize that, the flow rate is not constant in time because the process is nonstationary. At the very beginning and at the end there are low crowd pressures which make the flow rate very low for small values of v_d.

5.3. *Mean clogging delay*

Clogging delays were defined in Sec. 4.1. Here, in Fig. 3 the mean clogging delays as a function of v_d are shown.

It can be seen that this curve has the same tendency and the minimum is reached at the same v_d than the evacuation time curve (Fig. 1). This means that there is a direct relation between evacuation time and clogging delay.

5.4. *"Arch-clogging" correlation*

In Sec. 4.3, the concept of Blocking Cluster was introduced. In Fig. 4, we show a typical blocking cluster.

As the value of v_d is increased, the probability of appearance of a blocking cluster increases (see Fig. 5). This is due to the fact that as the value of v_d is increased particles can overcome the social force repulsion and then, they start interacting via granular forces. These granular forces can generate clusters which block the exit of particles.

In order to quantify the relationship between the presence of a blocking cluster and the appearance of a clogging delay, we define the "arch-clogging" correlation

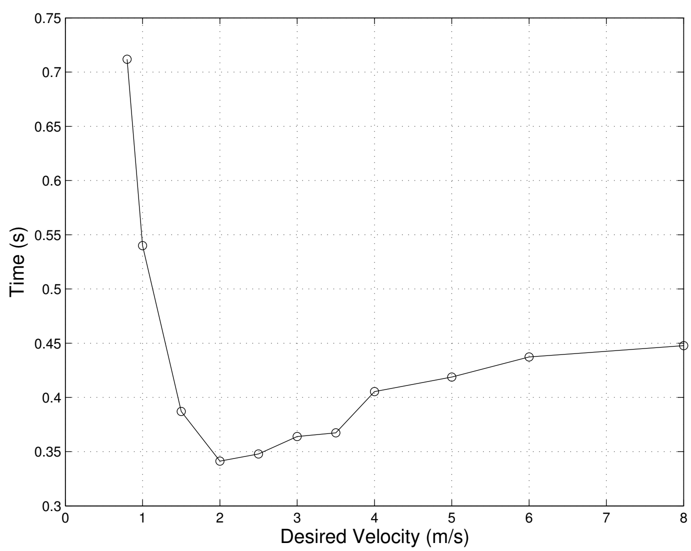

Fig. 3. Mean clogging delays for the 200 persons evacuated versus v_d.

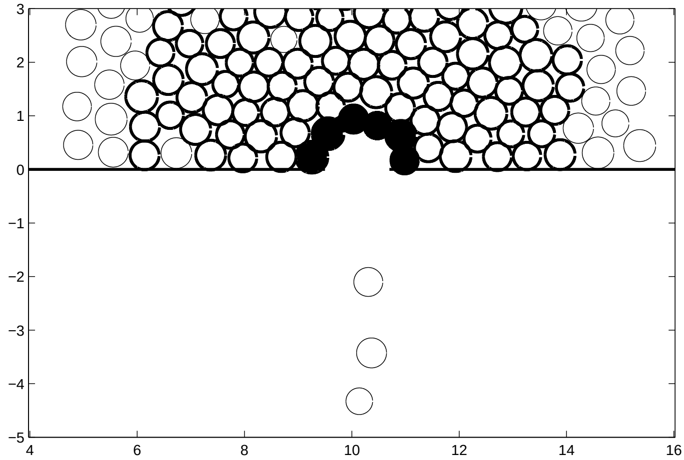

Fig. 4. A typical blocking cluster (black particles). Particles belonging to any arbitrary cluster > 1 are drawn with wider lines.

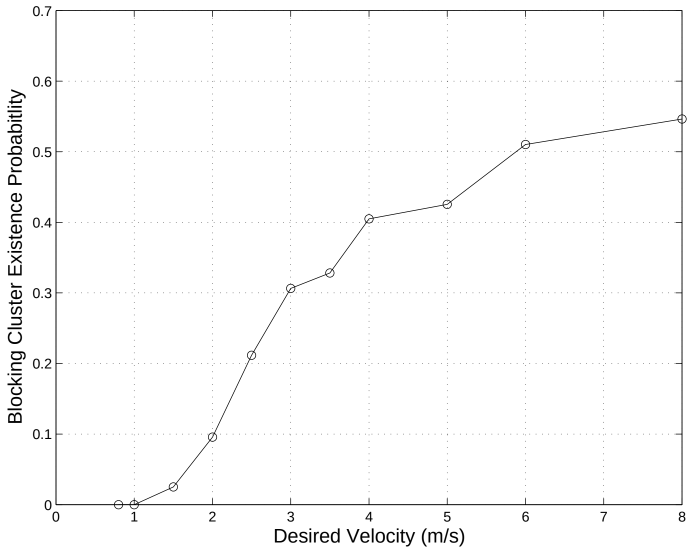

Fig. 5. Blocking cluster existence probability as a function of v_d.

coefficient as follows:

$$c_{ac} = \frac{1}{N} \sum_{cd=1}^{N} f(t_2^{bc}, t_1^{cd}, t_2^{cd}) \,, \quad (6)$$

where N is the total number of clogging delays in each run, t_2^{bc} is the time at which some arbitrary blocking cluster brakes down, t_1^{cd} is the time at which the associated clogging delay starts, and t_2^{cd} is the time at which this clogging delay finishes. "Associated" means that the first particle that exits the room at time t_2^{cd} (when the clogging delay finished) must be one of the particles that belonged to the blocking cluster broken at t_2^{bc}. The function f is such that:

$$\begin{aligned} f &= 1 \quad \text{if } t_1^{cd} \leq t_2^{bc} \leq t_2^{cd}\,, \\ f &= 0 \quad \text{otherwise}\,. \end{aligned} \tag{7}$$

We now present the results of the calculation of c_{ac}. Figure 6 shows the value of the c_{ac} coefficient for different clogging delay ranges.

The meaning of, for example, a value of c_{ac} of 0.6 is that the 60% of the clogging delays (in the range considered) were produced by blocking clusters and the remaining 40% are due to social clogging.

It can be seen that the correlation between the presence of a blocking cluster and a clogging delay is almost one for delays longer or equal to 2.3 s and v_d bigger than 2.0 m/s, which is the optimal velocity for evacuation. Below this velocity all "long delays" are due to social clogging.

For shorter clogging delays the competition between social clogging and blocking clusters is evident. In particular, for the shortest bin considered ($0.1 \leq cd \leq 0.3$) blocking clusters are responsible for at most 30% of the clogging delays.

From this analysis, it is clear why, above the threshold velocity v_{dt}, "Faster is slower". As the value of v_d is increased, the probability of appearance of a blocking cluster increases (see Fig. 5), which turns out to be strongly correlated to large clogging delays (see Fig. 6).

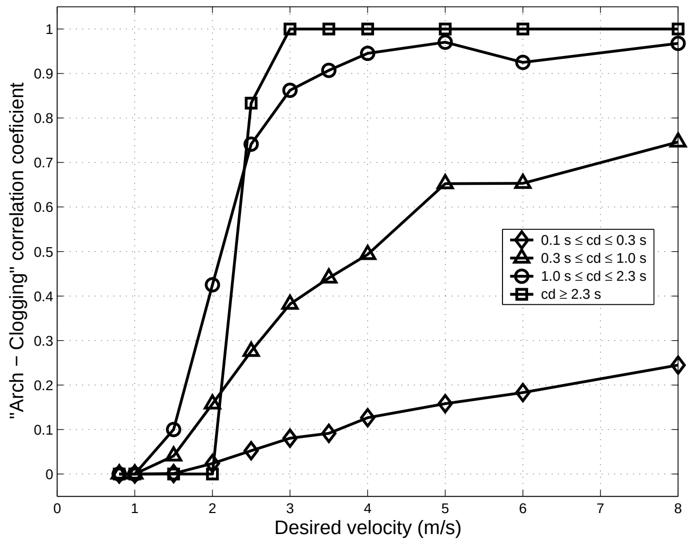

Fig. 6. Arch-clogging correlation coefficient, as defined in Eq. (6), versus v_d.

6. The Stationary Case

Since the nonstationary case limits our capacity of analysis, it is desirable to explore a stationary version of the problem. In the previous sections, we have shown that the mechanism responsible for the decrease of the efficiency of evacuation of the system for high v_d is the blocking cluster formation. This blocking cluster needs a bigger cluster as a substrate. Therefore, the most critical stage of the evacuation process is when large clusters are formed. This state of the system can last forever if outgoing particles are reinserted inside the room. In such a case the most relevant observable is the discharge curve. For the stationary case this curve has a constant slope (see Fig. 8) so the flow rate (number of particles leaving the room per unit time) is well-defined. Then, under steady state conditions, the variable that characterizes the evacuation performance of the system, for each v_d, is the flow rate.

6.1. *Flow rate versus desired velocity*

The state of the system which corresponds to most efficient evacuation, is characterized by the v_d which maximizes the flow rate of the system. As expected, the flow rate curve versus v_d has the same qualitative behavior as the evacuation time in the nonstationary case, displaying an extremum at an intermediate value of v_d. However, the value of v_{dt} is quantitatively different. In the stationary problem, $v_{dt} = 1.375$ m/s as can be observed in Fig. 7.

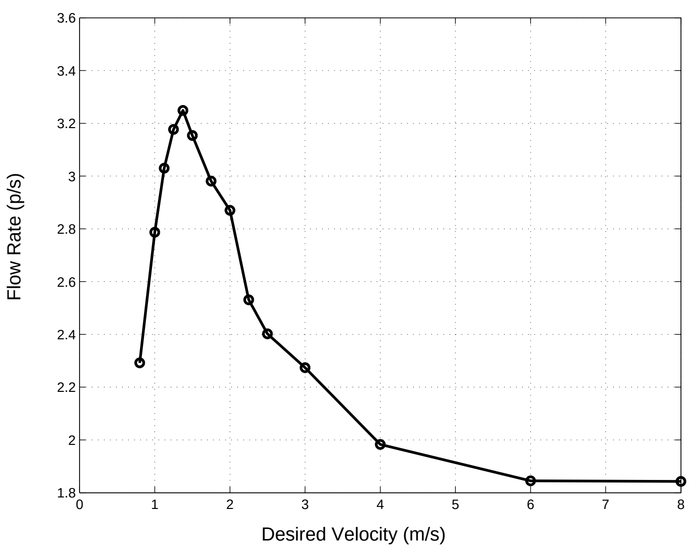

Fig. 7. Flow rate of the evacuation system as a function of v_d. The maximum is reached at $v_{dt} = 1.375$ m/s.

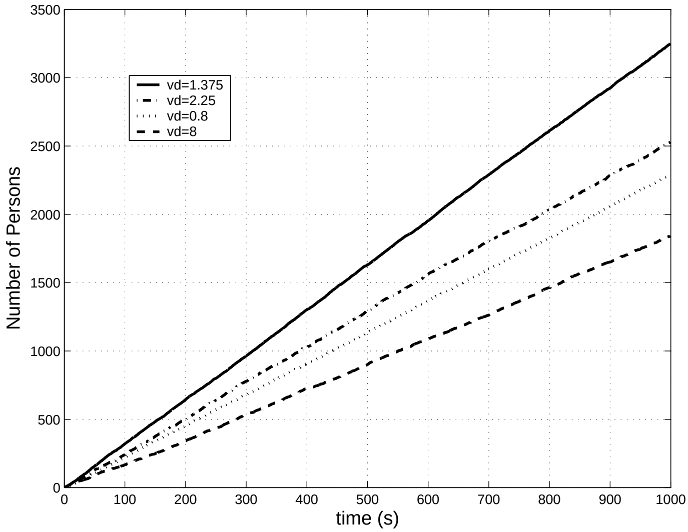

Fig. 8. Discharge curve for $v_d = 0.8$, 1.375, 2.25 and 8.0 m/s. Clogging delay is not evident in these curves due to the scale.

6.2. *Discharge curve*

In Fig. 8 the discharge curves for $v_d = 0.8$, 1.375, 2.25 and 8.0 m/s are shown.

In the stationary case, only one run of 1000 s is performed for each v_d. From these curves, the flow rate can be calculated.

6.3. *Granular cluster analysis*

Making use of the definition of granular cluster given in Sec. 4.2, we study the morphology of the system inside the room.

First, the cluster size distribution is analyzed for various values of v_d. In Fig. 9 we show such distributions for $v_d = 1.375$, 2.25, 2.5 and 3.0 m/s.

It can be seen that the shape of the distributions change from exponential (at low v_d) to U-shaped (for high v_d). In between, a power law one can be found. This suggests that a phase transition might be taking place.

Looking at the second moment of the distribution without the maximum cluster, (see Fig. 10) we see that it displays a sharp maximum at $v_d = 2.25$ m/s, a value at which the shape of the cluster size distribution is close to a power law one.

We then see that the value of v_{dt} at which the change of behavior of the flow rate takes place (the flow rate changes its tendency at $v_{dt} = 1.375$ m/s) corresponds to a cluster size distribution well inside the exponentially decaying region. In the next section, we explore the possible causes of the existence of an optimum v_d for evacuating the room.

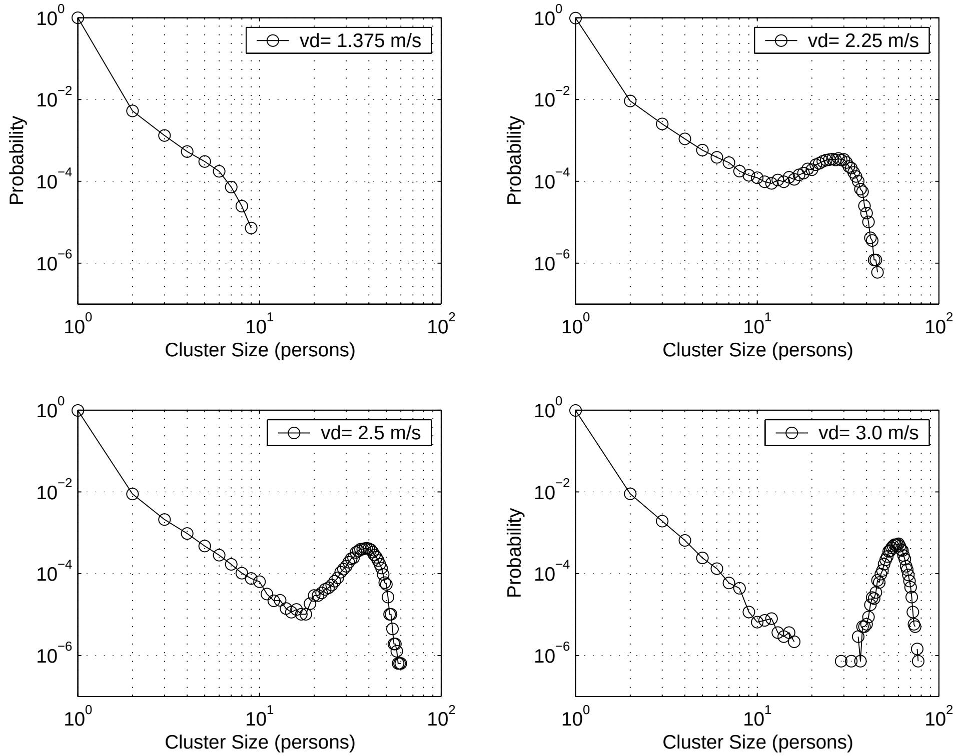

Fig. 9. Cluster size distributions for $v_d = 1.375$, 2.25, 2.5 and 3.0 m/s.

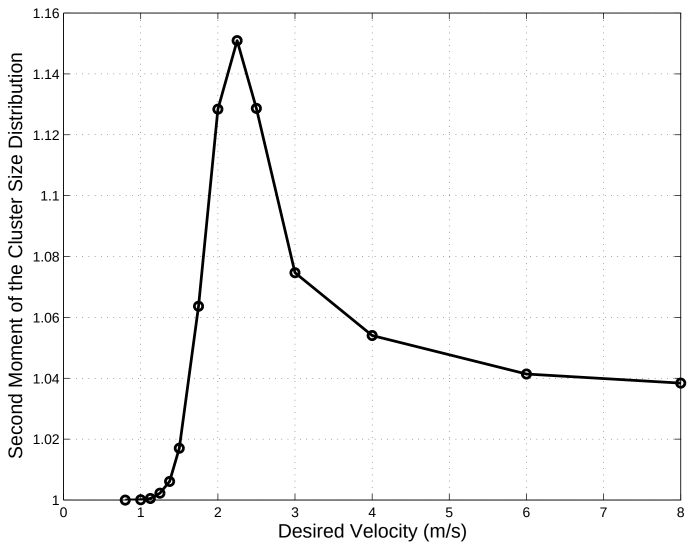

Fig. 10. Second moment of the cluster size distribution without the maximum cluster.

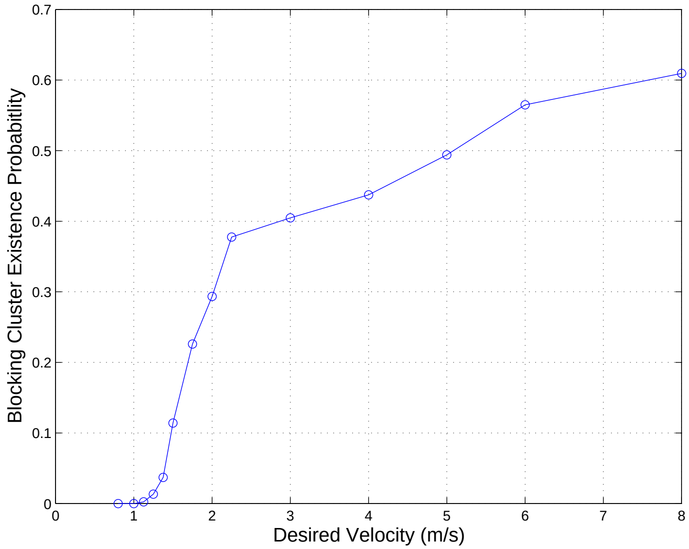

Fig. 11. Blocking cluster existence probability as a function of v_d.

6.4. *Total system forces analysis*

We start this section by displaying in Fig. 11 the probability of appearance of a blocking cluster as a function of v_d. As in the nonstationary case, this probability increases with the value of v_d.

It can be seen that this probability begins to be nonnegligible for values of v_d above $v_{dt} = 1.375$ m/s. It is clear that blocking clusters are responsible for the "faster is slower" effect above v_{dt}.

More information can be obtained if we analyze the total system forces.

Each particle has a unique desire force so the total desire force of the system at a given instant is

$$F_D^{Sys} = \sum_{i=1}^{N_p} |\mathbf{F}_{Di}| \,. \tag{8}$$

For the interacting forces (social and granular) the corresponding instant total system forces are given by the following equations:

$$F_S^{Sys} = \sum_{i=1}^{N_p} \sum_{j=1, j\neq i}^{N_p} A \exp\left(\frac{-\epsilon_{ij}}{B}\right) , \tag{9}$$

$$F_G^{Sys} = \sum_{i=1}^{N_p} \sum_{j=1, j\neq i}^{N_p} \{|-\epsilon_{ij} k_n - \gamma \mathbf{v}_{ij}^n| + |\mathbf{v}_{ij}^t \epsilon_{ij} k_t|\} g(\epsilon_{ij}) \,. \tag{10}$$

In Fig. 12, the variations of the mean system forces as a function of v_d can be observed. Figure 13 shows a zoom over the region of low values of v_d.

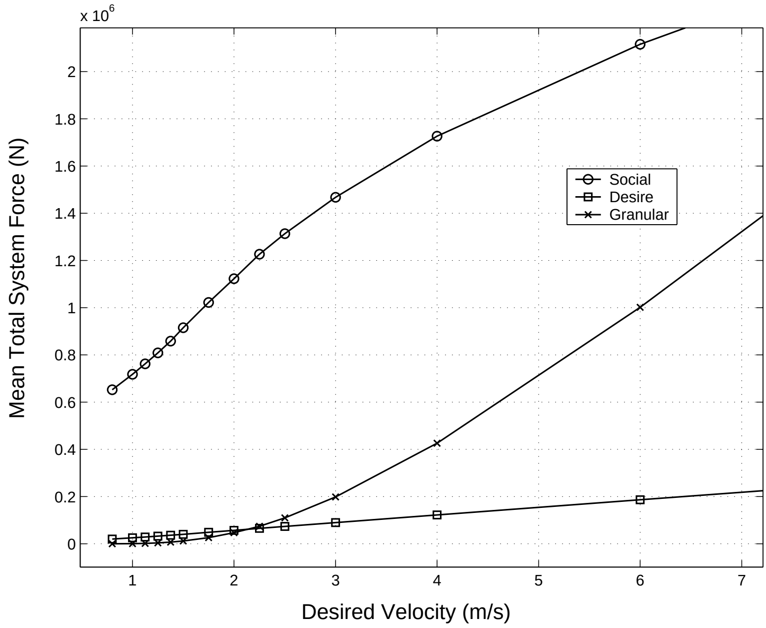

Fig. 12. Mean system forces (see Eqs. (8)–(10)) as functions of v_d.

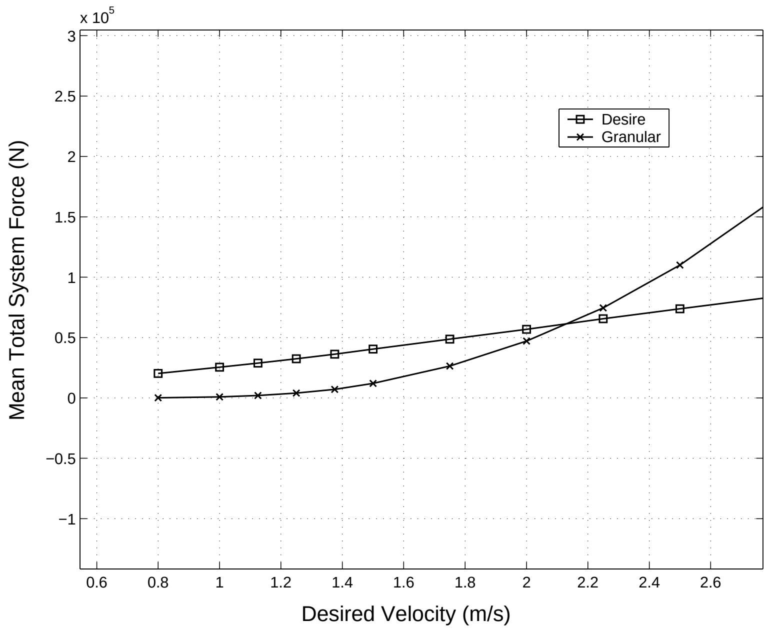

Fig. 13. Zoom of the previous figure into the low v_d zone.

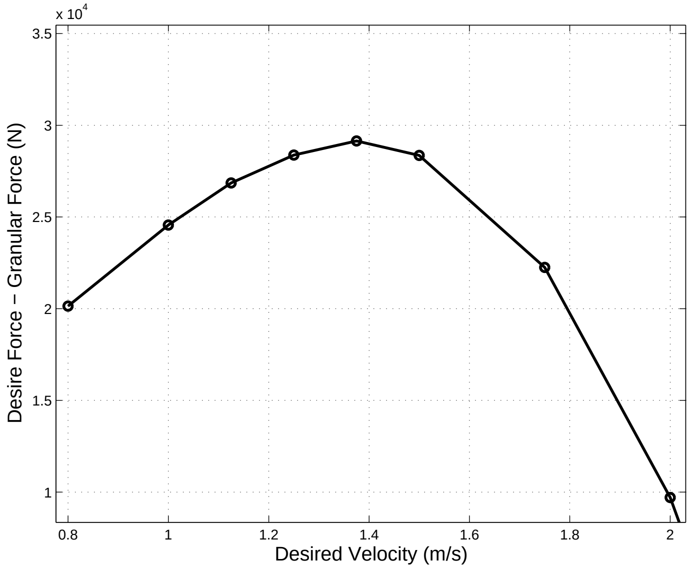

Fig. 14. Difference between the desire and granular mean system forces shown in the previous figure. The v_d that maximize this difference is equal to the v_{dt} at which the maximum evacuation efficiency is obtained.

This curves have two interesting points. The first one is the crossing point where the mean granular system force begins to be greater than the mean desired system force. This occurs near $v_d = 2.25$ m/s, the critical point from the granular cluster point of view (see Sec. 6.3).

The second interesting point can be better seen if we calculate the difference between the mean desire force $\langle F_D^{Sys} \rangle$ minus the mean granular force $\langle F_G^{Sys} \rangle$ (see Fig. 14).

It can be seen that this difference has a maximum at v_{dt} where the system reaches its maximum flow rate. This suggests that the optimum evacuation for the stationary case corresponds to a state in which a delicate relation between the average desire force and average granular force is attained. Taking into account that as the desired velocity is increased the granular force increases and that this last term does not behave linearly, the optimum evacuation is attained when the system reaches the maximal desired velocity that generates the minimal relative average granular force.

7. Conclusion

In this work we have focused on the microscopic analysis of the evacuation dynamics of self-driven particles confined in a square container with one exit door.

In the first part of this work we have fixed the number of particles to 200 and the width of the door has been taken as 1.2 m. It has been confirmed that the evacuation time (t_e) is a function of the desired velocity v_d. As already shown by

Helbing *et al.* we have found that there exists a threshold value of v_d such that below it, t_e is a decreasing function of v_d while above it, the tendency is reversed.

By analyzing the structure of the clusters that are formed in the system and introducing the concept of blocking clusters, we have been able to trace this change in behavior to the increase in the probability of long clogging delays. These long time clogging delays are correlated with the formation of blocking clusters.

From the dynamical point of view, the key effect is the increasing role of dissipative granular forces which become strong enough just above v_{dt} to make the probability of formation of clusters nonnegligible.

In the second part, we have focused on a stationary version of the problem in which particles are reinserted into the room once they have left it. In this case we have found that the optimum evacuation is attained when the difference between the average desire force and the average granular force is maximal. This suggests the following explanation of the change in the flow rate curve: Being the average desire force related to the capacity of displacement of the particles and the average granular force related to the capability of particles forming clusters, this would indicate that the optimal evacuation corresponds to the situation in which particles move as fast as they can producing a minimum number of clusters. This is a preliminary result that should be further investigated.

Acknowledgments

C. O. Dorso is a member of the "Carrera del Investigador" CONICET Argentina. D. R. Parisi is a postdoctoral fellow of the CONICET.

Figures 2, 3, 5 and 6 are reprinted from *Physica A* **354**, D. R. Parisi and C. O. Dorso, *Microscopic Dynamics of Pedestrian Evacuation* (2005), pp. 606–618, with permission from Elsevier.

References

1. S. Gwynne, E. R. Galea, M. Owen, P. J. Lawrence and L. Filippidis, *Building and Environment* **34**, 741 (1999).
2. Y. Tajima, K. Takimoto and T. Nagatani, *Physica A* **294**, 257 (2001).
3. Y. Tajima and T. Nagatani, *Physica A* **303**, 239 (2002).
4. T. Vicsek, A. Czirók, E. Ben-Jacob, I. Cohen and O. Shochet, *Phys. Rev. Lett.* **75**, 1226 (1995).
5. E. V. Albano, *Phys. Rev. Lett.* **77**, 2129 (1996).
6. A. Czirók, A.-L. Barabási and T. Vicsek, *Phys. Rev. Lett.* **82**, 209 (1999).
7. D. Helbing and P. Molnar, *Phys. Rev. E. Stat. Phys. Plasmas Fluids Relat. Interdiscip. Topics* **51**, 4282 (1995).
8. D. Helbing, I. Farkas and T. Vicsek, *Nature* **407**, 487 (2000).
9. D. R. Parisi and C. O. Dorso, *Physica A* **354**, 606 (2005).